Applied Catalysis B: Environmental 182 (2016) 59–67

Contents lists available at ScienceDirect

Applied Catalysis B: Environmental

journal homepage: www.elsevier.com/locate/apcatb

Photodriven formation of FeNi bimetallic nano-mixture accompanied with efficient hydrogen evolution under atmospheric oxygen

Chuan-Jun Wang[a], Yong Chen[a], Xiao-Jun Lv[a], Wen-Fu Fu[a,b,*]

[a] Key Laboratory of Photochemical Conversion and Optoelectronic Materials, CAS-HKU Joint Laboratory on New Materials, Technical Institute of Physics and Chemistry, Chinese Academy of Sciences, Beijing 100190, PR China
[b] College of Chemistry and Engineering, Yunnan Normal University, Kunming 650092, PR China

ARTICLE INFO

Article history:
Received 24 July 2015
Received in revised form 2 September 2015
Accepted 5 September 2015
Available online 9 September 2015

Keywords:
Binary-metal FeNi
Photogeneration
Photocatalysis
Hydrogen evolution
Oxygen toleration

ABSTRACT

Inexpensive and efficient catalysts which can promisingly operate under tolerant conditions are still urgently needed in the development of photocatalytic hydrogen evolution systems. Present work investigates the visible-light induced generation of bimetallic FeNi mixture with fluorescein (Fl) as photosensitizer in triethanolamine (TEOA) aqueous solution. FeNi NPs (NPs) *in situ* generated were found to be in intimate contact in the nano-mixture which upon formation performs as catalysts for photocatalytic hydrogen evolution in the same system under air atmosphere. Under bright LED light irradiation, the system with FeNi produced more than three times hydrogen than systems with same molar amount of single Fe or Ni component. Importantly, about two-fold higher hydrogen production activity compared with noble metal Pt catalyst under air atmosphere was observed. The work exhibited an economic and effective means of harnessing cheap bimetallics for tackling photocatalytic hydrogen evolution reactions. The mechanistic insights governing the photocatalytic processes and the factors leading to the enhanced hydrogen evolution activity were discussed.

1. Introduction

Extensive efforts have been devoted to photocatalytic water splitting as the prospect of converting solar energy into chemical energy through artificial photosynthesis is gaining increasing attention [1–4]. Hydrogen production can be realized in a multi-component system in the presence of a photosensitizer, a colloidal metal NPs or metal based complex catalyst and a small molecule sacrificial electron donor [5]. Tremendous works have dealt with the development of photosensitizers with improved charge transfer kinetics and the preparation of novel catalysts with optimized proton reduction abilities [6,7]. The development of earth abundant metal based complexes as proton reduction catalysts is in bloom in recent years [1,6,8–15]. However, preparation processes usually require intensive efforts and molecular complexes suffer from decomposition within hours of light irradiation [16–18]. Therefore, the stability and recyclability of catalysts should be reconciled with if application is to be considered. Most importantly, an economical photocatalytic system should also be active under tolerant conditions, preferably under air atmosphere which precludes the need for pre-degassing. Up until now, only a few works report hydrogen production systems functional under high levels of atmospheric oxygen [19,20].

Metal NPs were known to have good recyclability and adjustable size-controlled activities which can generally perform as stable catalysts during catalytic processes. Colloidal platinum is well known as effective hydrogen production co-catalyst [21,22]. However, the high cost and limited resource of Pt have led researchers in quest for inexpensive means of substitutes [1–6,8–15]. The practice of metal alloying for various catalytic reactions has witnessed flourishing developments in recent years [23–30]. Bimetallic NPs usually possess remarkably enhanced catalytic activities compared with their monometallic counterparts due to the existence of synergistic effect [25–27]. In addition, alloying is an economical means of reducing the usage of noble metals. For example, bimetallic NPs have been reported to exhibit dramatically enhanced electrocatalytic properties toward oxygen reduction reaction and methanol oxidation reaction [31–35]. Moreover, the studies of bimetallic NPs consisted of pure earth abundant elements would be more intriguing in a sense of cost-effectiveness and sustainable development. For instance, Carbon-coated FeNi composite as counter

* Corresponding author at: Key Laboratory of Photochemical Conversion and Optoelectronic Materials, CAS-HKU Joint Laboratory on New Materials, Technical Institute of Physics and Chemistry, Chinese Academy of Sciences, Beijing 100190, PR China. Fax: +86 10 62554670.
E-mail address: fuwf@mail.ipc.ac.cn (W.-F. Fu).

http://dx.doi.org/10.1016/j.apcatb.2015.09.017
0926-3373/

electrode were reported to exhibit more effective power conversion efficiency than Pt electrode in dye sensitized solar cells [36]. Dehydrogenation of Ammonia Borane with FeNi bimetallic NPs were also carried out in aqueous solution with enhanced activity [37].

Meanwhile, although light induced deposition of platinum NPs on the surface of semiconductors is well-established, there have been few investigations on photocatalytic hydrogen evolution catalyzed by cheap and stable NP catalysts, especially bimetallic or trimetallic alloys formed by a photoreduction method in an *in situ* generating system for hydrogen evolution under visible-light irradiation [38–41].

Our work herein report a visible-light-driven generation of FeNi binary nano-mixture as catalyst for *in situ* photocatalytic hydrogen evolution in a homogeneous system, with fluorescein (Fl) as light absorbing chromophore in alkaline triethanolamine (TEOA) solution under bright visible-light LED irradiation for the first time. The amount of hydrogen generated was carefully investigated under both degassed and air atmospheric conditions. It was found that when adding the same amount of the other cheap metal precursor (Fe^{3+} or Ni^{2+}) into the photocatalytic system, which would lead to the formation of FeNi bimetallic nano-mixture and a three-fold increase in the amount of hydrogen production compared to system with only one single metal element. Moreover, the hydrogen evolution with FeNi exhibited an approximately two-fold better performance than Pt catalyst under the same condition in air. The bimetallic NPs were characterized by transmission emission microscopy (TEM), X-ray diffraction (XRD) and energy dispersive X-ray analysis (EDX) etc., which in corroboration with control experiments showed that bimetallic FeNi was the active catalyst in the system. Furthermore, Sulfonated reduced graphene (SO_3-rGO) and SBA-15 was introduced into the system, which resulted in the formation of composite materials with dispersion of NPs on the surface of SO_3-rGO or inside the pore channels of SBA-15. The formation of nanohybrid catalysts has led to moderate to good performance of hydrogen evolution activity. The photocatalytic mechanism governing the formation of bimetallic NPs and their enhanced activity was presented.

2. Experimental

2.1. Assembly of photocatalytic system

In a typical reaction, a quartz tube containing $FeCl_3$ (5.0×10^{-5} M) and $NiCl_2$ (5.0×10^{-5} M) in TEOA (1.25%, v/v) aqueous solution (30 mL) was allowed to stirred under atmosphere, then 10 mg Fl (1.0 mM) was added into the resulting solution with vigorously stirring. For systems incorporating support materials, 5 mL (0.5 mg/mL) SO_3-rGO or 5 mg SBA-15 (commercially available, pore size about 8 nm) well dispersed in water were directly added into the photocatalytic system under stirring. Photocatalytic experiments were carried out under air-atmosphere, the tube containing the reaction solution was directly sealed without excluding air in the gas phase or solution. For photocatalytic experiments performed under inert atmosphere, the solution was deoxygenized with Ar for 30 min and then the tube was sealed with a rubber cap. The 10 samples were subjected to irradiation apparatus comprising LED light source (30×3 W, $\lambda \geq 420$ nm, 16 mW cm^{-1}) and magnetic stirrer, The generated hydrogen from the systems was measured at different time intervals by GC-14C (Shimadzu) which was equipped with a 5 Å molecular sieve column (3 m × 2 mm), thermal conductivity detector and Ar carrier gas. The amount of hydrogen was quantified by an external standard method. The turnovers were calculated based on the molar amount of added metal salts.

2.2. Characterization methods

The bimetallic NPs precipitated upon standing after irradiation were washed several times with deoxygenated ethanol, centrifuged and dried under an inert atmosphere. The dried NPs were used for XRD and X-ray photoelectron spectroscopy (XPS) measurements. For TEM measurement, the NPs were dispersed in deoxygenated ethanol solution. High resolution TEM (HRTEM) and EDS measurements were operated on a TEM (JEM 2100F) at an accelerating voltage of 200 kV. Electronic absorption spectra were recorded on a HITACHI U-3010 spectrophotometer. XRD spectra were collected on a Bruker D8 Focus under Cu-Kα radiation at (λ = 1.54056 Å). pH values were adjusted with a Model pH S-3C meter (Mettler Toledo FE20, China). XPS data were obtained by an ESCALa-b220i-XL electron spectrometer from VG Scientific using 300 W Al Kα radiations. The binding energies were obtained in reference to the C1s line at 284.8 eV. FT-IR spectra were collected on a Varian FT-IR Excalibur 3100 plus with the average of 32 scans with a resolution of 4 cm^{-1} from 4000 cm^{-1} to 500 cm^{-1}.

3. Results and discussion

3.1. Evaluation of photodriven hydrogen evolution with FeNi

In the first place, we investigated the influence of combining two kind of metal elements on the change of hydrogen production activity, with one or two metal salt components introduced into the photocatalytic system. It was found that all of the systems with two metal elements exhibited higher efficiency than that only contains one under the same experimental conditions (Fig. S1). Above all, the system with 0.05 mM $FeCl_3$ and 0.05 mM $NiCl_2$ showed the highest photocatalytic activity with more than 6.9 mL H_2 generated over 12 h of irradiation, which is more than 3 times than systems with either 0.1 mM $FeCl_3$ (2.1 mL H_2) or 0.1 mM $NiCl_2$ (2.1 mL H_2) added (Fig. 1A). In addition, control experiments revealed that neither nanoparticles nor any appreciable amount of hydrogen could be detected in the absence of any of the following components: Fl, TEOA, $FeCl_3$/$NiCl_2$ or light irradiation in the photocatalytic system (Fig. S2).

The *in situ* generation of Ni NPs from Ni(II) salt under intense light irradiation conditions have been frequently demonstrated in our works [38,41,42]. In the present system, the customer-designed LED device was equipped with 30 bright 3 w bulbs, which gave a focused light intensity of 16 mW cm^{-1} to the reaction tube. The formation of black naonoparticles can be observed in less than one hour of irradiation in the prior homogeneous aqueous solution. It is reasonable to assume that the dramatic enhancement in the hydrogen evolution efficiency was due to the synergistic effect between the *in situ* generated Fe and Ni NPs present in the same system. Further experiments were performed with different ratios of added $FeCl_3$ and $NiCl_2$ (Fig. 1B). When the concentration of Fe(III) and Ni(II) was 0.1 mM in total, the best hydrogen evolution activity was achieved at a Fe(III)/Ni(II) ratio of 1:1. Also, the concentration of sacrificial electron donor TEOA was varied to assess the influence on hydrogen evolution efficiency. The results showed that when decreasing the TEOA concentration from 10% to 5%, 2.5% to 1.25%, hydrogen evolution increased (Fig. S3). The low hydrogen evolution efficiency at high TEOA concentration was likely due to that metal ions are difficult to dissociate from M-TEOA complex, which would result in a longer induction period for the complete transformation of metal complex with TEOA ligand to metal NP catalysts. However, when further decreasing the concentration to 0.5%, the system exhibited a slightly lower efficiency with 3.0 mL H_2 obtained, which may be explained that the quick formation of free metal ions leads to the aggregation of particles formed fast.

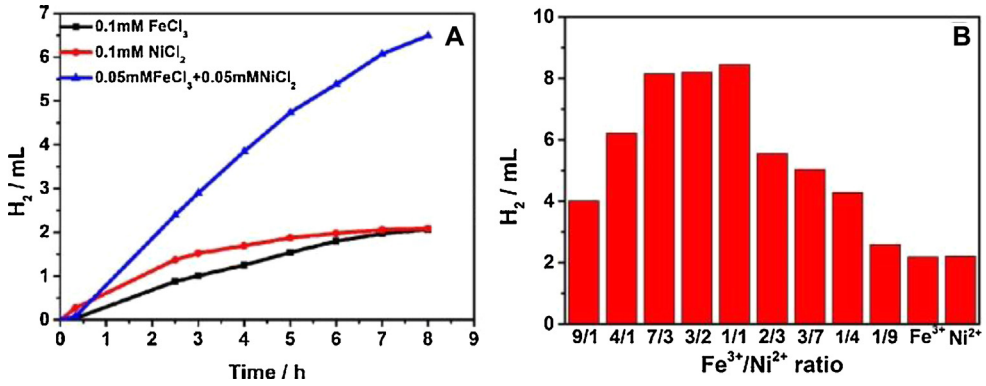

Fig. 1. (A) Photocatalytic hydrogen evolution in 30 mL degassed aqueous solution of Fl (1.0 mM), TEOA (1.25%), $FeCl_3$ (0.1 mM) or $NiCl_2$ (0.1 mM) or $FeCl_3$ (0.05 mM) + $NiCl_2$ (0.05 mM). (B) Photocatalytic hydrogen evolution under different ratios of added $FeCl_3$/$NiCl_2$ (0.1 mM in total), Fl (1.0 mM), TEOA (1.25%) in 30 mL degassed aqueous solution over irradiation 12 h. The total volume of the reaction tube was 60 mL. (LED light: $\lambda \geq 420$ nm, 30 × 3 W).

These results indicate an optimized concentration of TEOA (1.25%) for photocatalytic hydrogen evolution based on the proper balance of dissociation of M-TEOA precursor and coordiantion of metal ions. Moreover, we carried out photocatalytic experiments at different pH conditions (system without adjusting pH at 9.75). Over an irradiation time of 10 h, efficient hydrogen evolution activity can be observed over the pH range of 7.04–12.06, which was adjusted by 0.1 M HCl or NaOH. The highest efficiency at a pH value of 10.99 was achieved (Fig. 2A and B).

When extending the irradiation time at optimum pH values of 10.99 and 9.75, we came to find that the systems have prolonged lifetimes for hydrogen evolution. Hydrogen evolution proceeded for 36 h when it nearly reached a plateau (Fig. 2C). As demonstrated in literatures, *in situ* generated catalysts self-formed under photocatalytic conditions were generally stable against photodecomposition and the corresponding photocatalytic systems usually have prolonged lifetimes [14,15]. The catalysts that are self-generated, even if they are subjected to photodecomposition, can quickly re-assemble as long as the active components are still in existence. This recycling process was designated by the nature of the photoreduction system and the constant formation of the NPs was to be responsible that the system should have a prolonged lifetime.

When comparing the hydrogen production profiles at pH values of 10.99 and 9.75, we found that although the hydrogen evolution activity was slightly higher at pH 10.99 during the first 6 h of irradiation, system at pH 9.75 caught up in rate after 6 h and actually exceled in the amount of hydrogen producted after 18 h of irradiation. After 36 h of irradiation, 16.5 mL H_2 was generated in the system at pH 10.99, while 18.6 mL H_2 was obtained at pH 9.75.

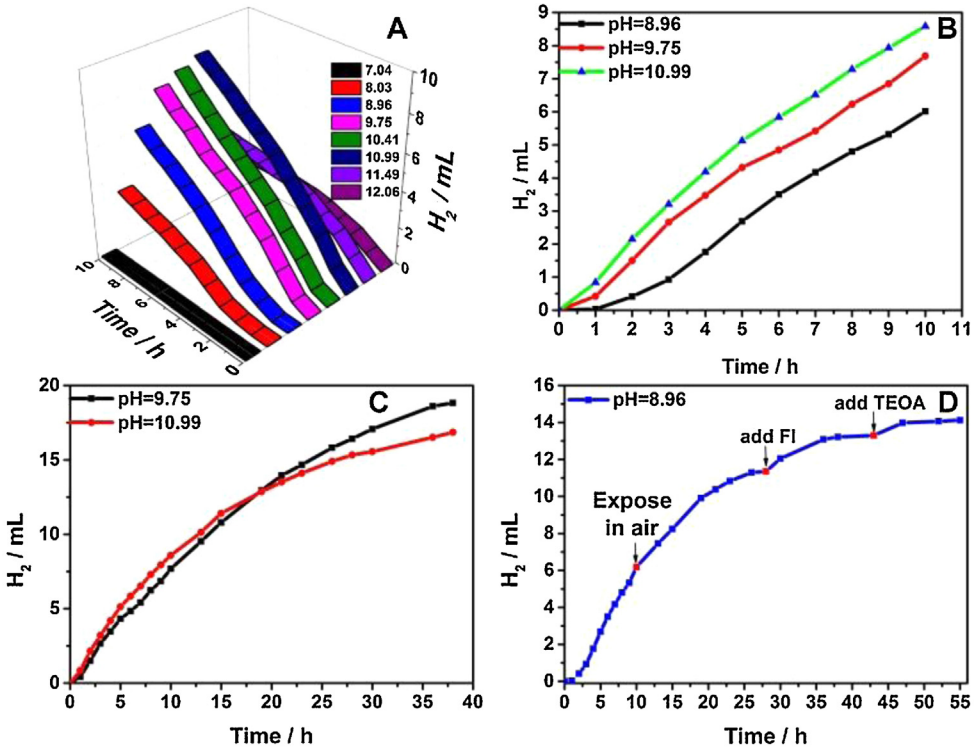

Fig. 2. (A) Photocatalytic hydrogen evolution with Fl (1.0 mM), TEOA (1.25%) and ($FeCl_3$ (0.05 mM) + $NiCl_2$ (0.05 mM)) in 30 mL degassed aqueous solution at various pH values for 10 h. (B) At pH 8.96, 9.75 and 10.99 for 10 h. (C) At pH 9.75 and 10.99 for 36 h of irradaition. (D) At pH 8.96, the reaction tube after 10 h of irradiation was exposed in air for 0.5 h and then sealed without degassing. Additional aliqouts of Fl and TEOA were added at 28 h and 43 h, respectively. The total volume of the reaction tube was 60 mL. (LED light: $\lambda \geq 420$ nm, 30 × 3 W).

Furthermore, Fl was introduced to the system at pH 9.75 when its hydrogen evolution activity reached a plateu at 38 h, the hydrogen evolution was partially resumed and continued for about 55 h (Fig. S4), which demonstrated that consumption of photosensitizer was responsible for the cease of activity at that time.

After irradaition for 10 h of the system at pH 8.96, the septum of the reaction tube was opened and the tube was left in open air for half an hour till it was occupied by air and then the tube was sealed again for irradiation. Photocatalytic experiments under constant stirring showed that hydrogen evolution could still be observed with gradual decrease in catalytic rate druing 10 h of irradiation. Adding a further aliquot of Fl at 27 h partially restored the activity up to 43 h, when the system again ceased producing hydrogen. After adding TEOA at 43 h, hydrogen evolution continued for another 10 h and a total amount of 14.1 mL H_2 was achieved (Fig. 2D).

Furtherfore, the photocatalytic system was evaluated under air-saturated at pH 9.75 and under atmospheric air. Fig. 3A demonstrates that photocatalytic hydrogen generation in the presence of atmospheric air displays decreasing activity over prolonged irradiation time. In comparison to the degassed system which produced 7.7 mL H_2 after 10 h of light irradiation, the air saturated system produced 4.8 mL H_2. Prolonging the irradiation to 24 h, the degassed system evolved 15 mL H_2 which gave a turnover numbers (TONs) value of 223 based on 0.05 mM Ni^{2+} + 0.05 mM Fe^{3+}, while air-affluent system gave 9 mL H_2 and a calculated TONs of 134 (Fig. 3B). It can be seen from these figures that the photocatalytic system maintained approximately 60 percent of the activity of the degassed system. Moreover, the photocatalytic hydrogen evolution in the presence of two metal components exhibited dramatically enhanced hydrogen evolution activity compared with monometallic ones. And it is an interesting and important fact that just by adding the same amount of the other metal salt precursor, both the activity and lifetime of the photocatalytic system should witness an enhancement of many times. (Fig. 3C) Furthermore, it is well-established that platimun NPs were among the most efficient catalysts for photocatalytic hydrogen evoution reactions and dramatic hydrogen evolution activity were previously reported based on Pt catalyst and modified molecular photosensitizers like iridium complexes [21]. However, most of these systems with Pt as catalyst as far as we know still have to operate under degassed conditions, as Pt is also well known to catalyze oxygen reduction reaction in the presence of oxygen [35]. Therefore, we have performed experiments to compare the photocatalytic activity of Pt and FeNi NPs in the present system. The results revealed that although FeNi ($FeCl_3$ (0.05 mM) + $NiCl_2$ (0.05 mM)) catalyzes less efficient hydrogen evolution than Pt (H_2PtCl_6 (0.1 mM)) under degassed conditions, an approxiamtely two fold higher activity of FeNi over Pt was observed in air saturated solutions under LED irradiation. (Fig. 3D). The excellent activity of FeNi bimetallics maybe attributed to their constantly *in situ* generation behavior in the photoreduction and hydrogen evolution system.

3.2. Characterization of bimetallic NPs

The *in situ* formed NPs precipitated upon standing were isolated and characterized by TEM, EDX, XRD and XPS measurements. The TEM image showed that the NPs generated were of small NPs closely attached to form an irregular mixture (Fig. 4A, S3 and S4). The nano-mixture was clearly of bimetallic nature, as evidenced by the corresponding High Angle Annular Dark Field Transmission Electron Microscopy (HAADF-TEM) image (Fig. 4B), and was distinctly different with NPs generated in systems with only one single metal component but under otherwise exactly the same conditions (Fig. S5 and S6). The selected area electron diffraction (SAED) displayed strong diffractions indicating of crystalline metallic nature of nano-mixture (Fig. 4A). This was further substantiated by the HRTEM image that showed the close contact of small NPs with sizes smaller than 5 nm and highly crystalline (Fig. 4C). The crystals had a measured spacing of 0.203 nm, which is consistent with the (1 1 0) crystal lattice plane (Fig. 4C) [38,39]. EDX analysis confirmed the existence of Fe and Ni in an atomic ratio of 1:1, which corresponds well with the ratio of added Fe^{3+} and Ni^{2+} precursor in the system and indicates complete transformation of all the metal components (Fig. 4E).

XRD of the bimetallic FeNi and individual NPs Fe or Ni generated under the photocatalytic conditions under air atmosphere were investigated separately (Fig. 4D). While the Fe NPs only showed the XRD diffraction peak of (1 1 0) crystal lattice of α-Fe, the Ni NPs displayed three peaks in the 2θ region that correspond to the cubic phase Ni (1 1 1), (2 0 0) and (2 2 0) planes (Fig. 4D). These results are in accordance with previous works of the Fe and Ni NPs *in situ* obtained under degassed conditions [38,39], which further demonstrated the photoreduction of metal salt precursor to metal NP catalyst of zero-valent nature under both inert and oxygen present conditions. In contrast, the experimental results revealed surprisingly that the FeNi nano-mixture *in situ* formed from added $FeCl_3$ and $NiCl_2$ precursor exhibited only one diffraction peak at 2θ around 44° under either N_2 or air atmospheric photoreduction conditions. Therefore, the result indicates that the presence of iron may either result in substantially narrowing of the size of generated Ni NPs or bring about an induced selective exposure of the (1 1 1) facet of Ni due to electron transfer from the more electronegative Fe(0) to Ni(0). Furthermore, FT-IR experiment confirmed the clean nature of the surface of generated NPs as after the cleansing process, no significant vibrations of functional groups of attached molecules were found upon detection (Fig. S7). The XPS analysis also revealed the presence of zero-valent metallic FeNi NPs in the mixture [43]. The detected Ni^{2+} and Fe^{3+} peaks are possibly due to the spontaneous oxidation of the highly active NPs in air during NP cleansing and collecting process (Fig. S8). The effective bimetallic catalyst generated through photocatalytic reaction is substantiated by control experiment with Fe_2O_3 directly added as catalyst in the same photocatalytic system. After longer irradaition time, the iron oxide was gradually reduced to iron NPs as confirmed by XRD, which resulted in the increasing hydrogen evolution activity (Fig. S14). In addition, the *in situ* generated FeNi bimetallic nanoparticles were collected and directly used as catalyst with Fl as photosensitizer and TEOA as sacrificial donor (Fig. S9). The system exhibited efficient hydrogen evolution activity under LED light, which ceased in darkness but resumed when light irradiation is further exerted. The system showed good stability over the two cycles of 24 h illumination (Fig. S9). These results revealed that hydrogen evolution was mediated by excited electron transfer from Fl* to the FeNi bimetallic catalyst. Therefore, we may safely conclude that the active catalyst for the observed robust hydrogen evolution under air atmosphere was the bimetallic FeNi nano-mixture *in situ* generated in the photocatalytic system.

3.3. Photocatalytic hydrogen production with in situ formed composites

Two-dimensional carbon based materials, especially rGO, are excellent catalyst scaffold to mediate electron transfer processes for photocatalytic reactions [44]. In addition, siliceous mesoporous materials like SBA-15 possess accessible mesoporous frameworks and suitable porosities that are beneficial for incorporation and modulation of NPs. In this regard, the addition of catalyst scaffold into the materials would lead to reasonably enhanced hydrogen evolution efficiency under light irradiation. We first introduced SO_3-rGO into the photocatalytic system containing all the other components prior to irradiation (Fig. 5A) [45]. The amount of hydrogen evolved was detected over time under different amounts of

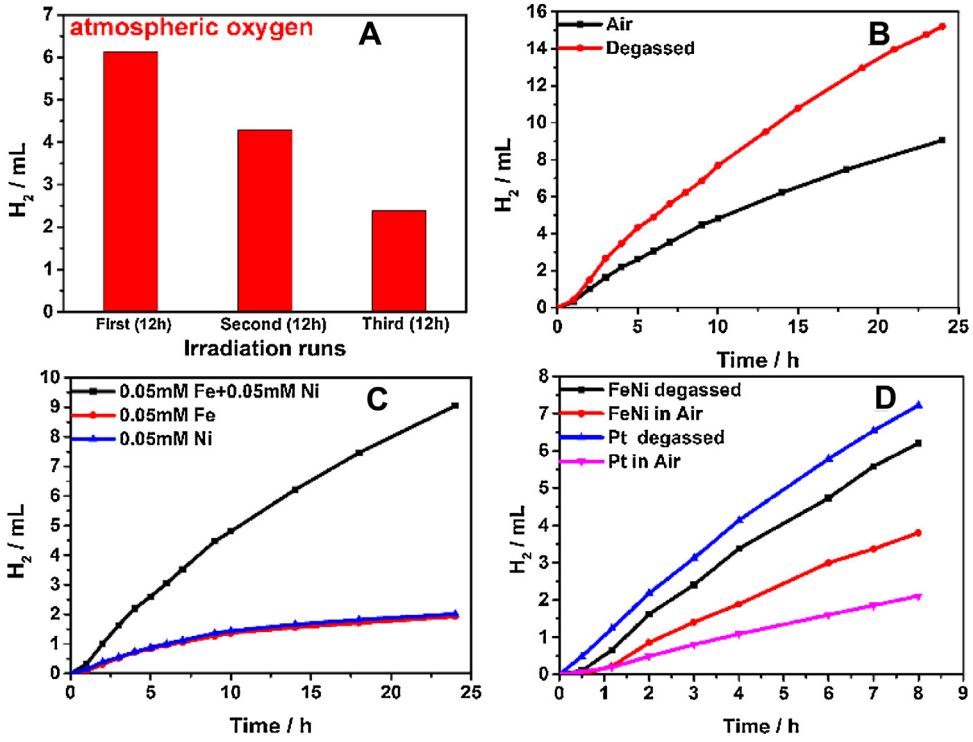

Fig. 3. (A) Photocatalytic runs with ($FeCl_3$ (0.05 mM) + $NiCl_2$ (0.05 mM)) in 30 mL aqueous solution in air saturated solution. (B) Hydrogen evolution under degassed and atmospheric oxygen. (C) Hydrogen evolution under atmospheric oxygen ($FeCl_3$ (0.05 mM) + $NiCl_2$ (0.05 mM) and $FeCl_3$ (0.05 mM) or $NiCl_2$ (0.05 mM). (D) Hydrogen evolution with added ($FeCl_3$ (0.05 mM) + $NiCl_2$ (0.05 mM) and H_2PtCl_6 (0.1 mM). All of the systems contain Fl (1.0 mM) and TEOA (1.25%), pH 9.75. (LED light: $\lambda \geq 420$ nm, 30×3 W).

added SO_3-rGO (1 mL to 6 mL, 0.5 mg/mL). The result revealed that system incorporating 5 mL (0.5 mg/mL) SO_3-rGO exhibited the best performance over a whole irradiation period of 20 h (Fig. S10). However, in comparison with system without SO_3-rGO, only moderate enhancement in photocatalytic activity was observed. Hydrogen evolution under air atmosphere was almost the same in the first three hours (1.85 mL *vs* 2.01 mL for system with SO_3-rGO), after which time the system with SO_3-rGO exhibited gradually enhancing efficiency than system without the support material (Fig. 5E). The only slightly increased activity maybe attributed to the dispersion effect of graphene, which reduced aggregation but in turn hampered the synergistic interaction between the Fe and Ni in the nano-mixture. HRTEM image of a NPs cluster on the surface of SO_3-rGO showed that the NPs were highly crystalline with measured lattice fringe of 0.203 nm, indicating the formation of metal NPs (Fig. 5B). This result was corroborated by further XRD analysis of the collected metal and sulfonated graphene composite material precipated after irradiation, which showed a clear diffraction peak at 2θ around 44°, same as the system which did not incorporate graphene support (Fig. S11).

When mesoporous SBA-15 (5 mg) was introduced into the photocatalytic system, hydrogen evolution also witnessed an increase in efficiency (Fig. 5F). After 13 h of light irradiation under the bright LED irradiation, 7.89 mL H_2 was produced in the system incorporating SBA, whereas only 5.91 mL was obtained in systems without the support material. It is reasonable to assume that with the relatively large pore size (around 8 nm) of the material, both the photosensitizer Fl and the metal TEOA precursor would be able to infiltrate into the channels of the material and thus form NPs within the channels, which due to the size-confinement and stabilizing effect would result in an increase in the hydrogen evolution activity. The proposition was substantiated by TEM experiments in Fig. 5C and D. A blank sheet of SBA-15 showed clear the empty channels of the mesoporous material under TEM experiments, with the pore size around 8 nm (Fig. 5C). After light irradiation in the *in situ* photoreduction of metal ions and photocatalytic hydrogen evolution system, the collected SBA-15 composite materials which were thoroughly cleansed by washing were found to be in dull black color, which was in sharp contrast to the snowy white pure SBA-15 added. TEM images showed that the pores of the material were filled with black NPs (Fig. 5D).

3.4. Induction period of hydrogen production

The photocatlytic process was proposed to be initially involving the dissociation of the metal-TEOA complex precursor to generate the active NPs. To provide proof to this supposition, the formation process of the NPs was investigated by analyzing the induction periods of hydrogen evolution at various pH values. As shown in Fig. 2 and S12, with the increase of the pH value, photocatalytic hydrogen evolution witnessed a decrease of the induction period for efficient hydrogen evolution. When the pH were increased to 11.45 and 12.06, the hydrogen evolution profiles of corresponding systems witnessed an actual disappearance of induction period. It is also interesting to note that quick formation of black naoparticles can be observed at higher pH values. The presence of the induction period also gives evidence that the M-TEOA complex was not an efficient molecular catalyst in the present system. Only when metal NPs were generated did we observe the efficient evolution of hydrogen, which gives evidence that nanostructured metal catalyst performed the role of hydrogen evolution in the system. The result was corroborated by the fact that when TEA was used as electron donor instead of TEOA, fast generation of metal NPs with efficient evolution of hydrogen was observed as metal oxides was readily present in the presence of TEA [39]. However, the lower photogenerating hydrogen activity at pH values of 11.49 and 12.06 should be ascribed to the low concentration of H^+ in the system (Fig. 2A).

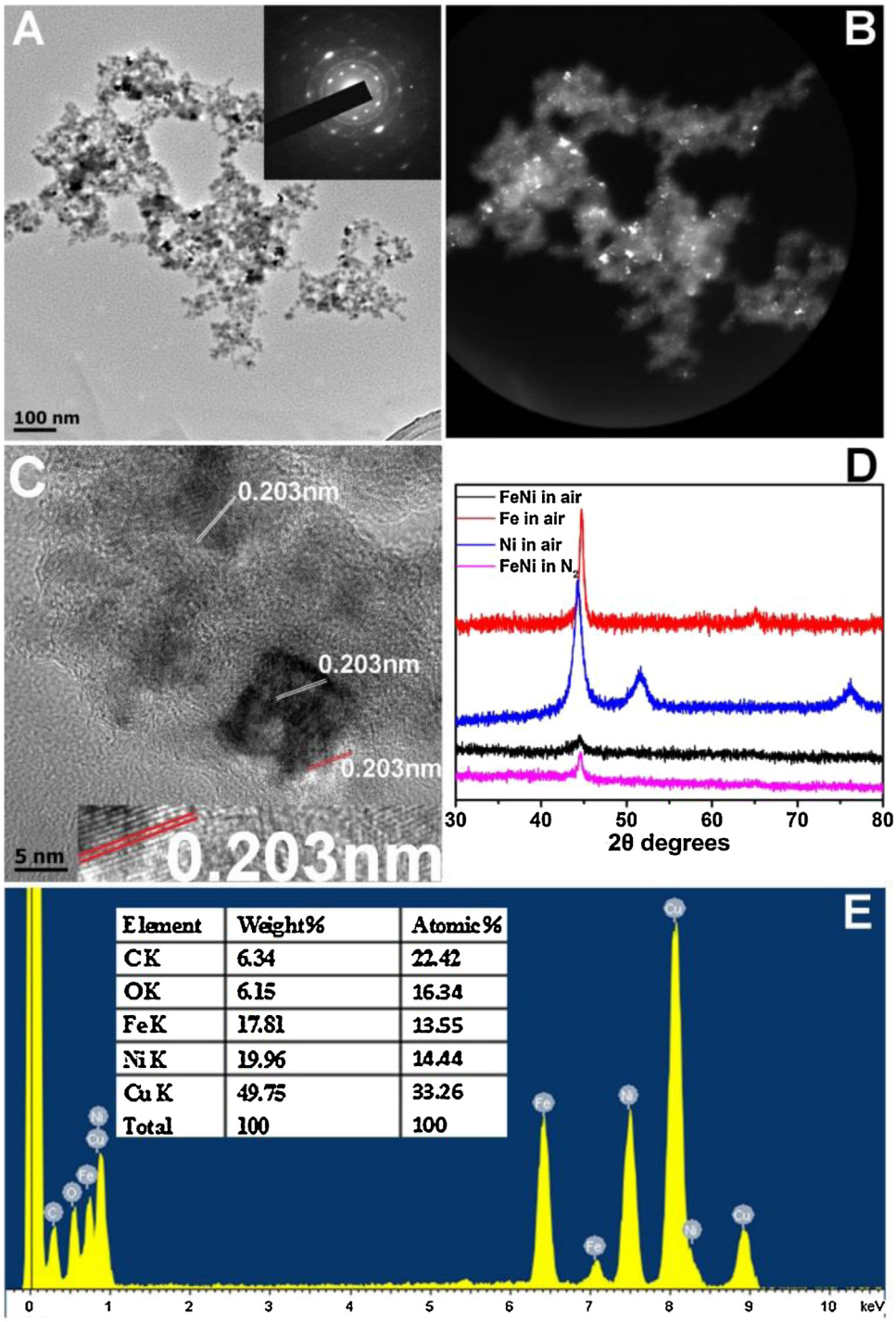

Fig. 4. (A) TEM image of *in situ* generated FeNi bimetallic mixture. Inset: SAED pattern. (B) HAADF-TEM (C) HRTEM image and (D) XRD of the Fe, Ni and FeNi mixture generated under air atmosphere or degassed conditions. (E) TEM-EDX of the generated FeNi mixture.

3.5. Formation of bimetallic FeNi NPs

Furthermore, the photocatalytic hydrogen evolution profiles incorporating bimetallic salts or monometallicl salt were carefully compared to shed light upon the photoreduction formation of metal NPs. According to Fig. 6A and Fig. S13 in Supplementary information, after 1 h of light irradiation, 0.097 mL H_2 was produced in the system with bimetallic ions added. However, this situation was changed when measuring the hydrogen evoled at 2 h, the bimetallic system excelled in the amount of hydrogen produced than both of the monometallic ones. The better performance of the bimetallic system was further confirmed by evaluating the hydrogen production at 3 h. The better performance of the Ni system at initial stage indicates the quick reduction of Ni^{2+} as demonstrated in our previous work that formation of nickel NPs can be detected by Dynamic light Scattering experiments in less than 10 min of irradiation [38]. While the photoreduction of Fe(III) was much slow and hydrogen evolution exhibited a much longer time of induction period in TEOA which had virtually no hydrogen evolution during that time [39]. However, after the first hour of irradiation, the almost simultane-

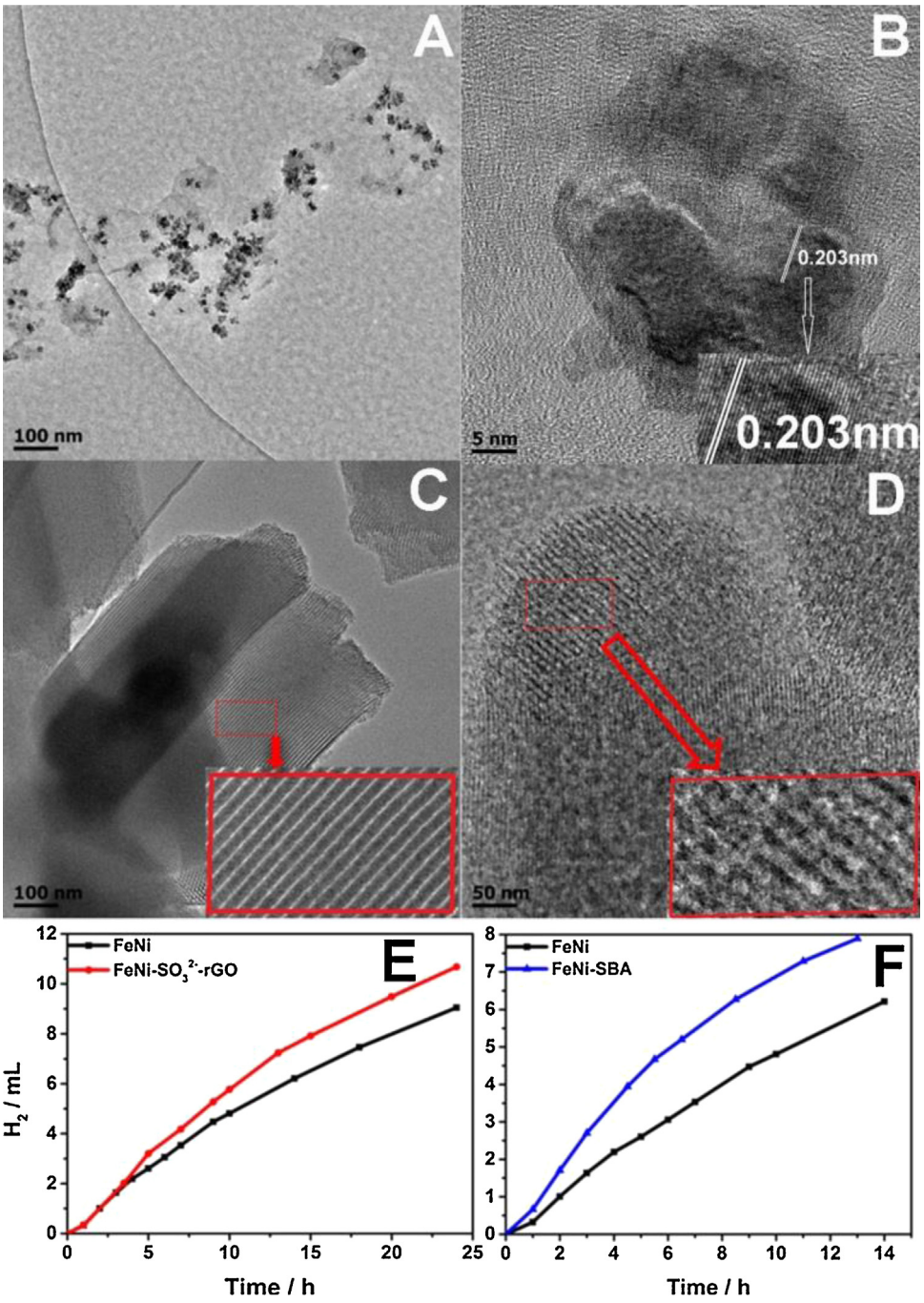

Fig. 5. (A) TEM image of FeNi NP self-deposited on SO_3^{2-}-RGO surface. (B) HRTEM of a NPs cluster on SO_3^{2-}-rGO. (C) TEM image of bare pieces of SBA-15 sheet. (D) TEM image the metal-SBA-15 composite material after irraiation. Inset: enlarged picture of the selected area showing the channels were filled with NPs. (E) Photocatalytic hydrogen production with and without SO_3^{2-}-rGO (5 mL, 0.5 mg/mL) or (F) 5.0 mg SBA-15 systems containing Fe^{3+}/Ni^{2+} (0.05 mM + 0.05 mM) and and Fl (1.0 mM) in 30 mL TEOA (1.25%) air saturated aqueous solution. LED light, $\lambda \geq 420$ nm, 30×3 W.

ous reduction of metal precursors produced bimetallic FeNi NPs in close contact which have resulted in the excelled performance over monometallic ones (Fig. 6A).

The arguement was further supported by the UV–vis absorption measurements after 12 h of light irradiation (Fig. 6B). The system incorpoating both Fe(III) and Ni(II) exhibited the highest Fl absorption after 12 h of irradaition, which demonstrated the better stabilizing effect of the bimetallic components for photosensitizers. In comparison, the absorption of Fl in iron based system showed the lowest Fl absorption. Our previous work have shown that Fl decomposed most fast in the initial hours of photoreduction process, while after the formation of metal NP catalysts when hydrogen evolution begins to take dominance, the decomposition rate of Fl is much slower as a result of the stabilizing interaction between the NPs and light emmitting chromophores [39,46]. Since the photoreduction induction period is the longest for the Fe based system, therefore the Fe based system showed the most consumption of the Fl absorption, while the FeNi system which exhibited the best

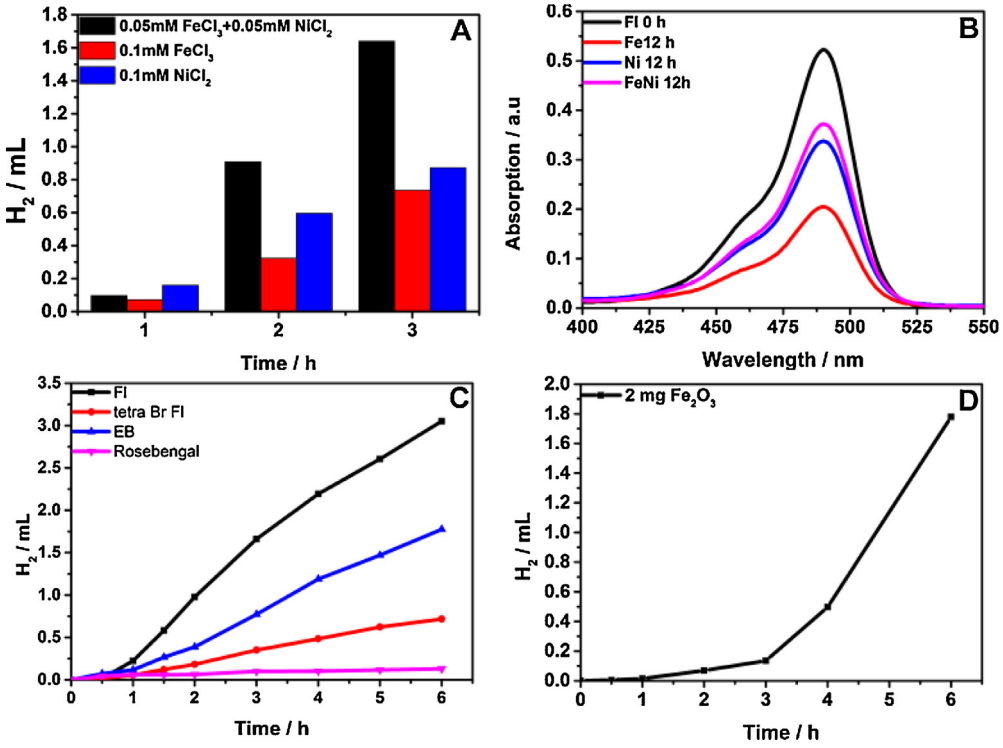

Fig. 6. (A) Comparison of photocatalytic hydrogen evolution in the initial 3 h of light irradiation. (B) Comparison of UV–vis absorption of Fl after 12 h of light irradiation. (C) Photocatalytic hydrogen evolution with various photosensitizers (1.0 mM). Conditions: Fl (1.0 mM), TEOA (1.25%) and ($FeCl_3$ (0.05 mM) + $NiCl_2$ (0.05 mM)) and $FeCl_3$ (0.1 mM) or $NiCl_2$ (0.1 mM) in 30 mL air saturated aqueous aolution. (D) Photocatalytic hydrogen evolution with Fl (1 mM), TEOA (1.25%) and Fe_2O_3 (2 mg) in 30 mL H_2O under air atmosphere. (LED light: $\lambda \geq 420$ nm, 30 × 3W). The total volume of the reaction tube was 60 mL.

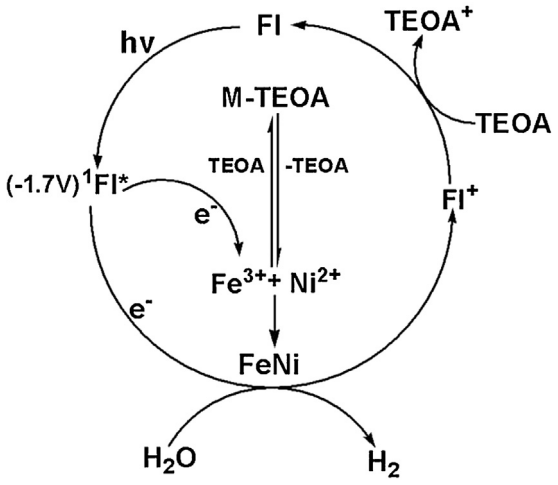

Fig. 7. Schematic illustration of photoreduction generation of FeNi bimetallic catalyst for H_2 production by oxidative quenching process.

performance for hydrogen evolution dispalyed the best stabilizing ability for Fl over 12 h of irradaition.

3.6. Proposed mechanism for hydrogen evolution in air

The hydrogen evolution activity under high levels of atmospheric oxygen conditions is also very intriguing and can be attributed to the oxidative quenching process of singlet electron transfer from excited state Fl* to metal components. In the first place, the sacrificial electron donor TEOA can quench triplet excited state of molecular photosensitizers but cannot quench the excited state fluroscence of Fl, which is of singlet nature (Fig. 7) [47]. However, NPs can quench the singlet fluorescence of Fl [39]. Therefore, the electron transfer process with Fl as photosensitizer was mediated by electron transfer from excited state Fl* to metal ions through oxidative quenching process for reduction to metal ions and also simultaneously to the generated NPs for the subsequent photocatalytic hydrogen evolution. Most of the previous works have used metal complex photosensitizers, which are usually of triplet excited state nature that are apt to be quenched by oxygen, the exploitation of Fl as photosensitizer and TEOA as eletron donor ensured the fast singlet electron transfer from the Fl* directly to catalysts, which presents certain advantage for excluding the influence of oxygen. The proposition was corroborated by control experiments with different halogenated fluroscein molecules as photosensitizers which showed that the best hydrogen evolution performance was achieved with Fl as photosensitizer, while the most inferior was obtained with Rosebengal which possesses four iodine on the fluroscein motif and is mostly of triplet excited state nature (Fig. 6C). However, the hydrogen evolution profiles in the presence of atmospheric air still did not match fully with that under degassed conditions. It is possible that the presence of oxygen in the aqueous solution may in some degree result in deactiviation of the active sites on metal NPs by oxidizing the surface of the NPs. Therefore, control experiments were performed with 2 mg Fe_2O_3 (commercially available, structure determined by XRD) added as catalyst in combination with Fl (1.0 mM) and TEOA (1.25%) in air saturated aqueous solution, the experimental result showed the presence of an induction period that had almost no hydrogen production activity during the first hour of irradiation, which confirmed that the metal oxide was not effective catalyst for hydrogen evolution in the present system. The hydrogen production increased dramatically and more and more with prolonging of irradiation from 2 h to 6 h (Fig. 6D). The result hints upon the photoreduction of Fe_2O_3 to Fe NPs, which is the real active metal catalyst. Furthermore, 10 mg Fe_2O_3 were also added in a system at the same photocatalytic conditions for 12 h LED irradiation under

air atmosphere, XRD experiment of the sample collected after 12 h have indeed revealed the emergence of the (1 1 0) diffraction peak of Fe besides that of the Fe_2O_3 (Fig. S14). It is therefore conclusive from hydrogen evolution (Fig. 6D) and the XRD results that the present system incorporating Fl and TEOA were able to transform metal oxide to metal NPs, which is the real highly active catalytst responsible for the robust hydrogen evolution activity under the present photocatalytic conditions.

4. Conclusion

The photoinduced generation of bimetallic FeNi nano-mixtures has been investigated in detail in alkaline aqueous solution incorporating organic photosensitizers as reducing agent under bright visible-light LED irradiation and the subsequent hydrogen evolution reaction under atmospheric air-saturated conditions with these *in situ* formed binary metal catalysts was observed. Highly efficient hydrogen evolution can be achieved with the bimetallic FeNi, which not only showed better performance compared with their monometallic counterparts but also demonstrated excelled activity than Pt NPs generated under the same reaction conditions in the presence of oxygen. Characterization of the NPs further confirmed the metallic nature of the close-contacted nano-mixtures. Once support materials like SO_3-rGO or SBA-15 was introduced into the system, *in situ* formed metallic-support composites display moderate to good enhancement of the photocatalytic activities. The photocatalytic mechanism governing the formation of the bimetallic mixtures and their enhanced activity was illustrated by following a series of induction period measurements and monitoring the corresponding absorption profiles. The singlet nature of the photosensitizer and the dominant oxidative quenching process when TEOA was used as sacrificial electron donor were proposed to be highly responsible for the photocatalytic hydrogen evolution in air. And the synergistic interaction between the Fe and Ni was proposed to be responsible for the enhance activity. This work demonstrates a feasible system for photocatalytic generation of bimetallic catalysts with earth-abundant metal components as catalysts for hydrogen evolution under air-saturated atmospheric conditions, which may also hold great promise for replacement of noble metal NPs for solar driven water splitting reactions.

Acknowledgements

This work was financially supported by the National Key Basic Research Program of China (973 Program 2013CB834804) and the Ministry of Science and Technology of China (2012DFH40090). We thank the Natural Science Foundation of China (NSFC Grant Nos. 21273257, 21471155, 21267025 and U1137606) and the Key Research Programme of the Chinese Academy of Science (Grant No. KGZD-EW-T05) for financial supports.

Appendix A. Supplementary data

Supplementary data associated with this article can be found, in the online version, at http://dx.doi.org/10.1016/j.apcatb.2015.09.017.

References

[1] V. Artero, M. Chavarot-Kerlidou, M. Fontecave, Angew. Chem. Int. Ed. 50 (2011) 7238–7266.
[2] V. Artero, M. Fontecave, Chem. Soc. Rev. 42 (2013) 2338–2356.
[3] J.L. Dempsey, B.S. Brunschwig, J.R. Winkler, H.B. Gray, Acc. Chem. Res. 42 (2009) 1995–2004.
[4] P. Du, R. Eisenberg, Energy Environ. Sci. 5 (2012) 6012–6021.
[5] A.J. Esswein, D.G. Nocera, Chem. Rev. 107 (2007) 4022–4047.
[6] W.T. Eckenhoff, R. Eisenberg, Dalton Trans. 41 (2012) 13004–13021.
[7] S. Fukuzumi, Y. Yamada, T. Suenobu, K. Ohkubo, H. Kotani, Energy Environ. Sci. 4 (2011) 2754–2766.
[8] Z. Han, W.R. McNamara, M.S. Eum, P.L. Holland, R. Eisenberg, Angew. Chem. Int. Ed. 51 (2012) 1667–1670.
[9] T. Stoll, M. Gennari, J. Fortage, C.E. Castillo, M. Rebarz, M. Sliwa, O. Poizat, F. Odobel, A. Deronzier, M.N. Collomb, Angew. Chem. Int. Ed. 53 (2014) 1654–1658.
[10] C. Orain, F. Quentel, F. Gloaguen, ChemSusChem 7 (2013) 638–693.
[11] X. Li, M. Wang, D. Zheng, K. Han, J. Dong, L. Sun, Energy Environ. Sci. 5 (2012) 8220–8224.
[12] H.N. Kagalwala, E. Gottlieb, G. Li, T. Li, R. Jin, S. Bernhard, Inorg. Chem. 52 (2013) 9094–9101.
[13] Z. Han, L. Shen, W.W. Brennessel, P.L. Holland, R. Eisenberg, J. Am. Chem. Soc. 135 (2013) 14659–14669.
[14] W. Zhang, J. Hong, J. Zheng, Z. Huang, J.S. Zhou, R. Xu, J. Am. Chem. Soc. 133 (2011) 20680–20683.
[15] Z. Han, F. Qiu, R. Eisenberg, P.L. Holland, T.D. Krauss, Science 338 (2012) 1321–1324.
[16] D. Hong, J. Jung, J. Park, Y. Yamada, T. Suenobu, Y.-M. Lee, W. Nam, S. Fukuzumi, Energy Environ. Sci. 5 (2012) 7606–7616.
[17] C.-F. Leung, S.-M. Ng, C.-C. Ko, W.-L. Man, J. Wu, L. Chen, T.-C. Lau, Energy Environ. Sci. 5 (2012) 7903–7907.
[18] P. Lei, M. Hedlund, R. Lomoth, H. Rensmo, O. Johansson, L. Hammarstrom, J. Am. Chem. Soc. 130 (2008) 26–27.
[19] F. Lakadamyali, M. Kato, N.M. Muresan, E. Reisner, Angew. Chem. Int. Ed. 51 (2012) 9381–9384.
[20] T. Sakai, D. Mersch, E. Reisner, Angew. Chem. Int. Ed. 52 (2013) 12313–12316.
[21] B.F. DiSalle, S. Bernhard, J. Am. Chem. Soc. 133 (2011) 11819–11821.
[22] R.P. Sabatini, T.M. McCormick, T. Lazarides, K.C. Wilson, R. Eisenberg, D.W. McCamant, J. Phys. Chem. Lett. 2 (2011) 223–227.
[23] R. Ferrando, J. Jellinek, R.L. Johnston, Chem. Rev. 108 (2008) 845–910.
[24] J. Gu, Y.W. Zhang, F.F. Tao, Chem. Soc. Rev. 41 (2012) 8050–8065.
[25] Z. Wei, J. Sun, Y. Li, A.K. Datye, Y. Wang, Chem. Soc. Rev. 41 (2012) 7994–8008.
[26] S. Guo, S. Zhang, D. Su, S. Sun, J. Am. Chem. Soc. 135 (2013) 13879–13884.
[27] M. Yamauchi, R. Abe, T. Tsukuda, K. Kato, M. Takata, J. Am. Chem. Soc. 133 (2011) 1150–1152.
[28] H.-L. Jiang, Q. Xu, J. Mater. Chem. 21 (2011) 13705–13725.
[29] Y. Wu, S. Cai, D. Wang, W. He, Y. Li, J. Am. Chem. Soc. 134 (2012) 8975–8981.
[30] G. Chen, Y. Zhao, G. Fu, P.N. Duchesne, L. Gu, Y. Zheng, X. Weng, M. Chen, P. Zhang, C.W. Pao, J.F. Lee, N. Zheng, Science 344 (2014) 495–499.
[31] L. Li, X. Chen, Y. Wu, D. Wang, Q. Peng, G. Zhou, Y. Li, Angew. Chem. Int. Ed. 52 (2013) 11049–11053.
[32] X. Xu, X. Zhang, H. Sun, Y. Yang, X. Dai, J. Gao, X. Li, P. Zhang, H.H. Wang, N.F. Yu, S.G. Sun, Angew. Chem. Int. Ed. 53 (2014) 12522–12527.
[33] X. Guo, Y. Zhang, C. Deng, X. Li, Y. Xue, Y.M. Yan, K. Sun, Chem. Commun. 50 (2014) 539–541.
[34] F. Saleem, Z. Zhang, B. Xu, X. Xu, P. He, X. Wang, J. Am. Chem. Soc. 135 (2013) 18304–18307.
[35] S. Guo, D. Li, H. Zhu, S. Zhang, N.M. Markovic, V.R. Stamenkovic, S. Sun, Angew. Chem. Int. Ed. 52 (2013) 3465–3468.
[36] X. Zheng, J. Deng, N. Wang, D. Deng, W.-H. Zhang, X. Bao, C. Li, Angew. Chem. Int. Ed. 53 (2014) 7023–7027.
[37] J.-M. Yan, X.-B. Zhang, S. Han, H. Shioyama, Q. Xu, J. Power Sources 194 (2009) 478–481.
[38] C.J. Wang, S. Cao, W.F. Fu, Chem. Commun. 49 (2013) 11251–11253.
[39] C.J. Wang, S. Cao, B. Qin, C. Zhang, T.T. Li, W.F. Fu, ChemSusChem 7 (2014) 1924–1933.
[40] S. Cao, C.J. Wang, X.J. Lv, Y. Chen, W.F. Fu, Appl. Catal. B: Environ. 162 (2015) 381–391.
[41] T. Simon, N. Bouchonville, M.J. Berr, A. Vaneski, A. Adrovic, D. Volbers, R. Wyrwich, M. Doblinger, A.S. Susha, A.L. Rogach, F. Jackel, J.K. Stolarczyk, J. Feldmann, Nat. Mater. 13 (2014) 1013–1018.
[42] H. Lv, W. Guo, K. Wu, Z. Chen, J. Bacsa, D.G. Musaev, Y.V. Geletii, S.M. Lauinger, T. Lian, C.L. Hill, J. Am. Chem. Soc. 136 (2014) 14015–14018.
[43] D. Li, M. Koike, L. Wang, Y. Nakagawa, Y. Xu, K. Tomishige, ChemSusChem 7 (2014) 510–522.
[44] S. Min, G. Lu, J. Phys. Chem. C 115 (2011) 13938–13945.
[45] H.-H. Zhang, K. Feng, B. Chen, Q.-Y. Meng, Z.-J. Li, C.-H. Tung, L.-Z. Wu, Catal. Sci. Technol. 3 (2013) 1815–1821.
[46] J. Enderlein, Appl. Phys. Lett. 80 (2002) 315–317.
[47] T. Lazarides, T. McCormick, P. Du, G. Luo, B. Lindley, R. Eisenberg, J. Am. Chem. Soc. 131 (2009) 9192–9194.